International Journal of Mass Spectrometry 303 (2011) 220–224

Contents lists available at ScienceDirect

International Journal of Mass Spectrometry

journal homepage: www.elsevier.com/locate/ijms

Reactions of positive ions with ClN_3 at 300 K

Nicole Eyet[a,b,d], Keith Freel[b,c], Michael C. Heaven[c], A.A. Viggiano[b,*]

[a] Department of Chemistry, St. Anselm College, 100 Saint Anselm Drive, Manchester, NH 03102, USA
[b] Space Vehicles Directorate, Air Force Research Laboratory, 29 Randolph Road, Hanscom Air Force Base, MA 01731-3010, USA
[c] Chemistry Department, Emory University, Atlanta, GA 30322, USA
[d] Institute for Scientific Research, Boston College, USA

ARTICLE INFO

Article history:
Received 25 June 2010
Received in revised form 3 February 2011
Accepted 4 February 2011
Available online 18 February 2011

Keywords:
Chlorine azide
Proton affinity
Ionization potential
Kinetics
Rate constants
Branching ratios

ABSTRACT

The kinetics of eighteen positive ions with chlorine azide (ClN_3) have been studied using a selected ion flow tube (SIFT). These measurements allowed for the estimation of both the ionization energy, >930 kJ mol^{-1} (>9.6 eV), and the proton affinity, 713 ± 41 kJ mol^{-1}, of chlorine azide. Reaction rate constants have been determined. Product ions have been identified, and quantified when synthetic complications allowed. In addition, general reaction trends have been observed. A reaction coordinate diagram for the novel reaction of N^+ with ClN_3 is discussed.

Published by Elsevier B.V.

1. Introduction

Halogen azides, in particular ClN_3, have recently been a source of significant interest. While their explosive nature has been a deterrent to an in-depth study of their reactivity [1], interest in their applications has renewed importance. Theoretical studies have predicted a cyclic N_3 isomer resulting from photodissociation [2–4]. This N_3 isomer could potentially be used to synthesize larger nitrogen heterocycles, which may be exploited as energy storage materials, propellants, or detonators. Consequently, several studies of the photodissociation of ClN_3 have been carried out. Two distinctive internal mode energy distributions have been observed for the N_3 fragment, where the higher energy product appeared to be consistent with predictions for cyclic N_3 [5,6].

Photodissociation studies have also observed the production of $NCl(a^1\Delta)$ [7]; this molecule is isoelectronic with $O_2(a^1\Delta)$. Like $O_2(a^1\Delta)$, $NCl(a^1\Delta)$ can be used in iodine lasers [8,9] where energy is transferred from the excited NCl molecules to I_2. This chemically driven process is preferable to the use of $O_2(a^1\Delta)$ as $NCl(a^1\Delta)$ is product of gas precursors, whereas the production of $O_2(a^1\Delta)$ through a chemical reaction involves bubbling Cl_2 though a solution [10–13].

Given the potential applications of ClN_3, knowledge of its reactivity is desirable. Until recently, the only ionic property of ClN_3 known was its ionization potential determined by photoionization [14,15]. In order to further understand the thermochemical properties of ClN_3 we have undertaken studies of a variety of plasma reactions. Recently, we have published the kinetics of electron attachment to ClN_3 and a study of the reactions of ClN_3 with a variety of negative ions [16,17]. In the latter study the electron affinity of ClN_3 was determined to be 2.48 ± 0.2 eV. Here, we extend this work by examining the reactions with positive ions. The kinetics of ClN_3 with eighteen positive ions has been investigated, allowing for general reaction trends and thermochemistry to be determined. In particular we focused on reactions that allow for the ionization potential and proton affinity to be determined. The experimental study is complemented by theoretical studies of the energetics, and the reaction coordinate for an interesting reaction was determined. It was necessary to also study the reactivity of these ions with Cl_2 since unreacted Cl_2 from ClN_3 preparation entered the flow tube.

2. Experimental

These experiments were carried out using the selected ion flow tube (SIFT) at the Air Force Research Laboratory. Since this instrument has been described in detail elsewhere [18] only a brief description will be provided here. Ions were produced in a moderate pressure ion source. The desired reactant ions were selected by a quadrupole mass filter and injected through a Venturi inlet

* Corresponding author. Tel.: +1 781 377 4028; fax: +1 781 377 1148.
E-mail address: afrl.rvb.pa@hanscom.af.mil (A.A. Viggiano).

1387-3806/$ – see front matter. Published by Elsevier B.V.
doi:10.1016/j.ijms.2011.02.004

into a reaction flow tube where they were thermalized by collisions with helium buffer gas. Neutral reagents were added through an inlet 59.0 cm upstream from the sampling orifice. Depletion of the parent ion and appearance of the product ions were monitored using a quadrupole mass filter coupled to an electron multiplier.

Each reactant ion was prepared from an appropriate precursor. O_2^+ and O^+ ions were formed from O_2, H_3O^+ was formed from water, and NO_2^+ was formed from NO_2. $CH_3OH_2^+$ was formed from methanol and produced by injecting the dimer $(CH_3OH)_2H^+$ with sufficient energy to dissociate the cluster; CH_3^+ resulted when injecting this cluster with even higher energy. C^+ and CO^+ were formed from CO. Ar^+ was made from Ar; N_2^+ and N^+ were produced from N_2. SF_5^+ and SF_3^+ were produced from SF_6. SO^+ and HSO_2^+ were produced from SO_2 with and without the addition of water, respectively. CS_2^+ was produced from CS_2.

Chlorine azide was produced [17] according to Eq. (1)

$$NaN_3(s) + Cl_2(g) \xrightarrow{H_2O} ClN_3(g) + NaCl(s) \quad (1)$$

Approximately 5 g of sodium azide was distributed on a 50 cm^3 piece of glass wool. The glass wool was sprayed with distilled water, rolled up and placed in a glass vessel. This vessel was maintained at 0 °C using a recirculating chiller. A mixture of 10% chlorine gas in helium flowed through the vessel, at a known rate, producing ClN_3. Residual water was removed by passing the flow through a trap containing Drierite at 7 °C. The flow of ClN_3 then passed though a Perkin-Elmer Lambda 10 UV-Vis Spectrometer, where the spectrum taken over the range 190–300 nm was compared to the known ClN_3 absorption spectrum. Absolute concentrations were determined in real time by measuring the absorbance at λ_{max} = 205.6 nm. The reaction yield varied between 20 and 100%, with typical yields of greater than 70% for these measurements. More details concerning ClN_3 production are given elsewhere [17].

In some cases, unreacted Cl_2 was introduced into the flow tube along with ClN_3. To account for this complication, reaction rate constants and product ion branching ratios were measured for the ions interacting with Cl_2. Any contributions in the ClN_3 data from reactions with Cl_2 were removed. Additionally, a small amount of H_2O was not removed by the Drierite and introduced into the reaction flow tube with the ClN_3 flow. O_2^+ and O^+ reactions were carried out before Drierite was added to the reaction setup, resulting in a higher amount of water contamination. Knowledge of the reactivity of all reactant ions with H_2O was used to determine possible contributions to the rate constants and product ion branching ratios. This is discussed in more detail below. While it would be possible to form HN_3 in the reactor, no evidence of the molecule being produced has been seen using this technique [19]. Specifically in this experiment, no contamination of the flow was observed; our UV–Vis spectrum showed no evidence of the presence of this species ($\lambda_{max}(HN_3)$ = 193 nm) within our detection limit. Data were collected under lower resolution conditions in order to minimize mass discrimination. The semi-logarithmic decays of Cl_2 and ClN_3 were observed to be linear in all cases.[1] Decay of the primary ion was ~20% for the slowest reactions and up to 80% for faster reactions. Due to the difficulties of this experiment we assign large error bars of ±35% to the reaction rate constants and ±40% of the minor products to the product ion branching ratios, if numbers are assigned. Fig. 1 shows a typical data set for the reaction of SO^+ with ClN_3. The decline in the SO^+ is somewhat small but due to the ClN_3 production technique, but this is the most we can generate without significantly upping the impurity levels. The total ion signal remains constant indicating that the kinetics are adequate for measuring the rate constant. Numerous products are formed and secondary chemistry is sorted out in the normal SIFT manner by plotting fractional product concentration vs. ClN_3 concentration.

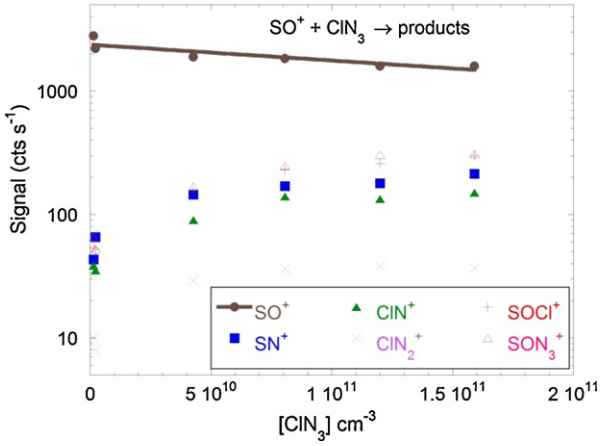

Fig. 1. Kinetic plot for the reaction of SO^+ with ClN_3. Products appear at zero concentration because some ClN_3 leaks through the generator even without Cl_2 flow.

Electronic structure calculations were carried out using the Gaussian 03 [20] suite of programs. Calculations of the ionization energy and the proton affinity were carried out using G3 theory [21], as it has been shown to provide accurate thermochemical information. Structures and energies in the reaction coordinate diagram were determined using the B3LYP hybrid density functional theory [22,23] with a 6-311+G(d) basis set.

Collisional efficiencies describe the fraction of collisions that result in a reaction (eff = k/k_{col}). The collisional rate constants (k_{col}) are calculated using parameterized trajectory collision rate theory. The dipole moment and polarizability were calculated using B3LYP/6-311+G(d). The dipole moment was determined to be 0.5363 D; the polarizability was determined to be 5.42 × 10^{-24} cm^3.

3. Results and discussion

3.1. Thermochemistry

Reactions used to bracket the ionization energy of ClN_3 are given in Table 1. ClN_3^+ was not observed as a product of any reaction. This observation is consistent with a past photoionization study [14] in which NCl^+ was observed to be produced at the lowest photon energy, a result of dissociative ionization ($ClN_3^+ \rightarrow NCl^+ + N_2$, $\Delta H_{rxn} < 27$ kJ mol^{-1}) [24]. The present determination of the ionization energy (IE) of ClN_3 is consistent with this previous determination. NO^+ and NO_2^+ were found not to react with ClN_3, which suggests that the IE of ClN_3 is greater than the IE of either NO or NO_2, making the IE > 930 kJ mol^{-1} (>9.6 eV). The majority of ions with higher IE's result in the formation of NCl^+; SF_5^+ was the species with the lowest IE to react to form NCl^+. This indicates that the IE may be near to that of SF_5 but the possibility that a reaction forming NCl^+ and other neutral products (rather than forming NCl^+ from dissociative charge transfer) cannot be ruled out. Reactant ions whose corresponding neutral molecules have ionization energies greater than 930 kJ mol^{-1} (9.6 eV) react via dissociative charge transfer, producing NCl^+. These results are consistent with a previous determination of the IE of 961 ± 2 kJ mol^{-1} (9.97 ± 0.02 eV) [14].

The proton affinity (PA) of ClN_3 was estimated; the reactions studied are given in Table 2. G3 calculations give three stable structures of $HClN_3^+$ shown in Fig. 2 – the proton can be attached to the

[1] We observed reactions with contaminant Cl_2 for reactions with O_2^+, H_3O^+, Ar^+, C^+, CO^+, N^+, N_2^+, SF_5^+, and SF_3^+. Reactions with contaminant H_2O were observed with O_2^+, $CH_3OH_2^+$, C^+ and O^+.

Table 1
Reaction rate constants, reaction efficiencies, and product ion branching distributions measured at 300 K for reactions used to determine the ionization energy of ClN_3.[a]

Reaction	Ionization energy (eV)[b]	Rate constant (10^{-10} cm^3 s^{-1})	Efficiency	Ionic products	Branching ratio
$Ar^+ + ClN_3$	15.76	<20	<1	NCl^+	
				Cl^+	
				N_3^+	Major
$N_2^+ + ClN_3$	15.58	<20	<1	NCl^+	Major
				Cl^+	
				ClN_2^+	
$N^+ + ClN_3$	14.53	17	0.9	NCl^+	0.7
				N_3^+	0.2
				Cl^+	0.1
				ClN_2^+	Trace
$CO^+ + ClN_3$	14	<10	<0.8	Cl^+	
				N_3^+	
				CCl^+	Major
				ClN_2^+	
$O^+ + ClN_3$	13.6	<40	<1	N_3^+	
				NCl^+	Major
$SO_2^+ + ClN_3$	12.35	5.6	0.5	$SOCl^+$	Trace
				NCl^+	0.8
				Cl^+	0.2
$O_2^+ + ClN_3$	12.07	15	1	NCl^+	
$C^+ + ClN_3$	11.2	<20	<1	NCl^+	Major
$SO^+ + ClN_3$	10.29	8.1	0.6	$SOCl^+$	0.2
				SON_3^+	0.2
				$SONCl^+$	0.3
				SN^+	0.2
				ClN_2^+	Trace
				NCl^+	0.1
$CS_2^+ + ClN_3$	10.073	6.8	0.6	$CSCl^+$	0.3
				CS_2N^+	0.7
$CH_3^+ + ClN_3$	9.84	27	1	CNH_2^+	0.9
				HN_3^+	0.1
$SF_5^+ + ClN_3$	9.6	0.13	0.01	NCl^+	Major
				SF_5ClN^+	
$NO_2^+ + ClN_3$	9.586	N/R	<0.001		
$NO^+ + ClN_3$	9.264	N/R	<0.001		
$SF_3^+ + ClN_3$	8.18	0.001	0.001	SF_2Cl^+	

[a] Reactions for which the neutral was not 100% pure have rate constants and branching ratios given as upper limits. Major products are defined as the ionic product in greatest abundance as a result of the reaction. See text for more detail.
[b] Taken from the NIST Webbook.

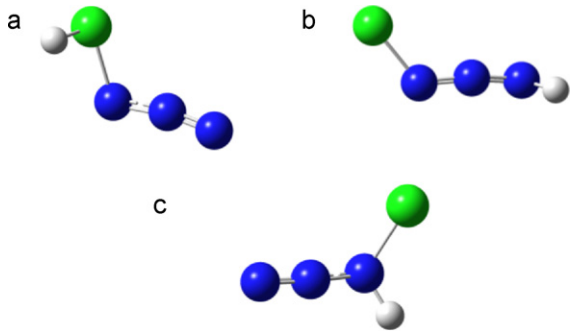

Fig. 2. Stable structures of $HClN_3^+$.

Cl (2a), to the N closest to the chlorine atom (2c), or to the N furthest from the Cl atom (2b), but not on the central N. The PA of isomer 2a is calculated to be 587 kJ mol^{-1}. The PA of isomer 2c is calculated to be 637 kJ mol^{-1}. The PA of isomer 2b is 703 kJ mol^{-1}. Proton transfer should occur when the proton affinity of ClN_3 is greater than the proton binding energy of the ion. Rapid, moderately efficient (35%), non-dissociative proton transfer was observed in the reaction with HSO_2^+, indicating the PA(ClN_3) > 672 kJ mol^{-1}. Comparing this measurement to computations reveals that the most stable form of $HClN_3^+$ was produced. While $HClN_3^+$ is not observed in reactions of ClN_3 with H_3O^+ and $CH_3OH_2^+$, the dissociative proton transfer product, HN_3^+, is observed. In the reaction with H_3O^+, this is not the major product channel, and the reaction is inefficient with only 8% of collisions resulting in a reaction. The inefficiency of the reaction suggest that the transfer of the proton is thermoneutral or even endothermic. At this level, we also cannot rule out that HN_3 con-

Table 2
Reaction rate constants, reaction efficiencies, and product ion branching distributions measured at 300 K for reactions used to determine the proton affinity of ClN_3.[a]

Reaction	Proton binding energy (kJ mol^{-1})[b]	Rate constant (10^{-10} cm^3 s^{-1})	Efficiency	Ionic products	Branching ratio
$CH_3OH_2^+ + ClN_3$	754	0.21	0.01	HN_3^+	
$H_3O^+ + ClN_3$	691	1.3	0.08	NCl^+	0.5
				HN_3^+	0.5
$HSO_2^+ + ClN_3$	672	4.2	0.35	$HClN_3^+$	0.1
				NCl^+	0.8
				Cl^+	0.1

[a] Reactions for which the neutral was not 100% pure have rate constants and branching ratios given as upper limits. Major products are defined as the ionic product in greatest abundance as a result of the reaction. See text for more detail.
[b] Taken from the NIST Webbook.

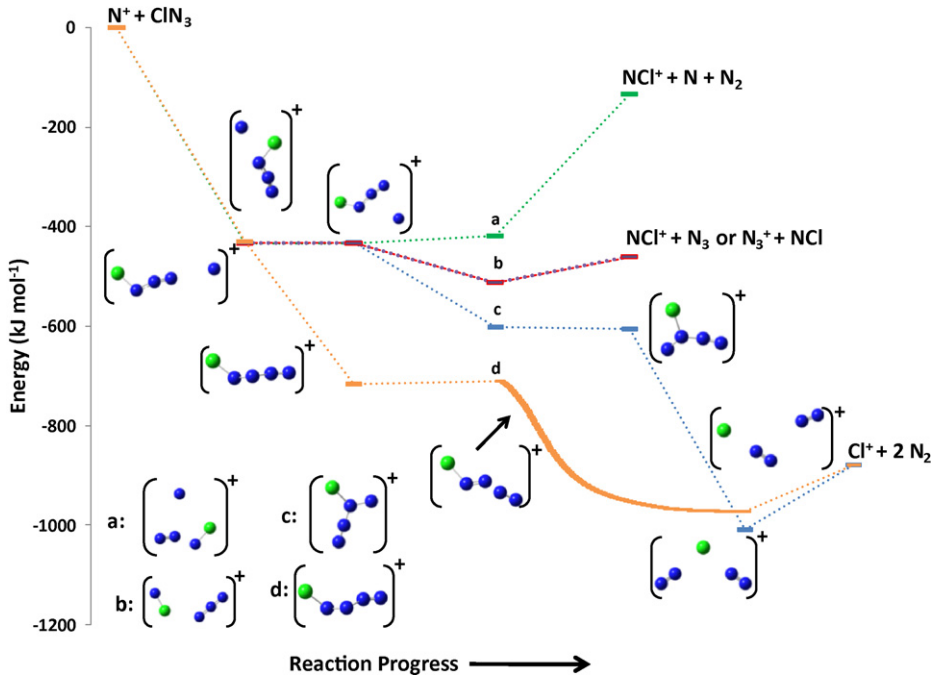

Fig. 3. Reaction coordinate diagram for the reaction of ClN_3 with N^+.

tamination below our detection limit was involved. This indicates that the PA of ClN_3 is approximately equal to that of H_2O. While the reaction of $CH_3OH_2^+$ does produce HN_3^+, this reaction is very inefficient (1%) suggesting proton transfer is an endothermic process. To be conservative, we bracket the PA to be 713 ± 41 kJ mol^{-1}, between CH_3OH and SO_2.

3.2. Reactivity

The general reactivity of ClN_3 with positive ions has been investigated in the course of determining the thermochemical properties of the molecule. However, because many of the positive ions involved in this study react with impurities inherent in the ClN_3 generation (Cl_2 and H_2O, which are difficult to completely trap) often only generalizations can be made about their reactivity. For conditions where products of these contaminant reactions were observed, product ion branching ratios could not be accurately determined, and instead only major products have been identified. Rate constants for these reactions are reported as upper limits, since the additional reactions add to the total depletion rate. In instances where Cl_2 and H_2O did not interfere substantially, reaction rate constants and product ion branching ratios are reported. O^+ and O_2^+ reactions were carried out before Drierite was added to the reaction setup. This resulted in a slightly higher water contamination, leading to an impossibly high rate constant for the reaction with O^+.

A few overarching trends could be gathered from analyzing the identity of the product ions. Often NCl^+ was produced in large abundance. Many reactions produced multiple species, a result of the fact that ClN_3 has a high energy content. Cl^+, N_3^+, and ClN_2^+ were produced in a number of the reactions. The reaction with SO^+ was notable in that six different products were produced, none with an abundance of more than 30%. A number of somewhat unusual ions were formed, including $CSCl^+$ and CS_2N^+ from CS_2^+, as well as $SONCl^+$ and SON_3^+ from SO^+. $SOCl^+$ resulted from reactions of both SO^+ and SO_2^+.

NCl^+ was a product for fourteen of the sixteen cations that did react. This product is a result of dissociative charge transfer, at least in a number of cases (see below). Additionally, reactions with ions having an ionization energy of greater than 1180 kJ mol^{-1} (12.2 eV) resulted in the formation of either Cl^+ or N_3^+, or both, likely also due to dissociative charge transfer.

For reactions of ClN_3 with negative ions, incorporation of oxygen into the product ions was observed. This is not the case for reactions of ClN_3 with positive ions. In contrast, reactions with isovalent sulfur-containing ions, with the exception of HSO_2^+, formed product ions containing sulfur. These sulfur containing product ions also incorporate either chlorine or nitrogen. If the production mechanism for these ions involves direct attachment, then the ions interact with neutral ClN_3 at several sites. G3 computations of the neutral species predict the Mulliken charges on the chlorine atom and the first and third nitrogen atoms to be negative, giving at least two likely places of attack for the positive ion.

Eight of the eighteen reactions proceeded with an efficiency of greater than 70%. Six reactions occurred very inefficiently: NO^+ and NO_2^+ did not react, and SF_3^+, SF_5^+, $CH_3OH_2^+$, and H_3O^+ reacted with efficiencies of less than 10%. In general, the cations in Table 1 with the highest ionization energies reacted more efficiently than those with lower ionization energies. No trend emerges when comparing proton binding energies, from Table 2, to overall reactivity.

While the number of reactions and products is too large for a comprehensive theoretical study, we have calculated the reaction coordinate diagram for $N^+ + ClN_3$, as an interesting case. It is shown in Fig. 3. The solid bars represent stationary points along the reaction coordinate; the solid portion of the orange line is a calculated internal reaction coordinate. The dashed lines are simply to guide the eye. This reaction provides a novel example of a reaction in which spin states are relevant. With few exceptions, it has been experimentally observed for spin allowed reaction pathways to be faster than spin forbidden ones [25–27]. We provide one possible set of reactions which include spin allowed pathways only. The ground state of N^+ is a triplet. That is, all intermediates and transition states reported here are also triplets, as well as the several ionic products (Cl^+, N_3^+). While it is possible spin forbidden pathways also play a role in these reactions, they are not addressed here.

NCl^+ can be produced as a result of dissociative charge transfer; this pathway is not shown in the diagram. For the reactive pathways two possible transition states with nearly identical energies are calculated. In one, N^+ attacks the lone pairs on the chlorine; it is also possible for the ion to attack the N-terminus of the chlorine azide molecule. These complexes are >400 kJ mol^{-1} more stable than the reactants. Attack on the Cl then proceeds by several pathways on a relatively flat part of the potential. The next step involves a small barrier that is essentially the rotation of the stable complex. At this point three pathways are accessible. Two simple paths have the complex separating as NCl^+ and N_3 (purple line, 70% including dissociative charge transfer), or as $N_3{}^+$ and NCl (red line, 20%). The ionization energies of the two radicals are nearly identical, making these pathways appear superimposed in the figure. Attack on the Cl end of the molecule can also proceed through a different transition state to form $NCl^+ + N + N_2$ (green line). Formation of Cl^+ can be explained from either initial transition state. The blue trace shows the production of $Cl^+ + 2N_2$ from an initial attack of on the Cl. The orange trace shows the production of $Cl^+ + 2N_2$ from an attack on the N-terminus of the molecule. (For interpretation of the references to color in this text, the reader is referred to the web version of this article.)

The solid, non-dashed portion of the orange line represents a calculated internal reaction coordinate. While we have been unable to locate a stable intermediate or product ion complex for the formation of $ClN_2{}^+$, the fragment is observed on the IRC; the structure is given in Fig. 3 and its initial appearance is designated with an arrow. It is presumed that a shallow minimum would be present if the calculations were carried out using a higher level of theory. It is also possible that $ClN_2{}^+$ is a result of a spin forbidden reaction pathway not calculated here. Both explanations would be consistent with the production of only trace amounts of $ClN_2{}^+$.

4. Conclusion

The reactivity of a variety of positive ions has been observed with chlorine azide, ClN_3. This reactivity allowed for the estimation of both the ionization energy, >930 kJ mol^{-1} (>9.6 eV), and the proton affinity, 713 ± 41 kJ mol^{-1}, of chlorine azide. The large energy content in the reactant has resulted in a large variety of ions produced. The one novel reaction coordinate, for $N^+ + ClN_3$ was calculated. Initial attack of the ClN_3 could occur at either end of the molecule. All products of this reaction can be explained using spin allowed pathways.

Acknowledgements

We are grateful for the support of the Air Force Office of Scientific Research for this work. K.F. acknowledges support from the National Research Council Fellowship Program. N.E. is under contract (FA8718-04-C-0055) to the Institute for Scientific Research of Boston College. We thank Raymond Bemish for helpful discussions concerning electronic structure calculations.

References

[1] W.J. Frierson, J. Kronrad, A.W. Browne, J. Am. Chem. Soc. 65 (1943) 1696.
[2] P. Zhang, K. Morokuma, A.M. Wodtke, J. Chem. Phys. 122 (2005) 014106.
[3] D. Babikov, P. Zhang, K. Morokuma, J. Chem. Phys. 121 (2004) 6743.
[4] I.S.K. Kerkines, Z. Wang, P. Zhang, K. Morokuma, J. Chem. Phys. 129 (2008) 171101.
[5] N. Hansen, A.M. Wodtke, J. Chem. Phys. A 107 (2003) 10608.
[6] N. Hansen, A.M. Wodtke, S.J. Goncher, J.C. Robinson, N.E. Sveum, D.M. Neumark, J. Chem. Phys. 123 (2005) 104305.
[7] N. Hansen, A.M. Wodtke, A.V. Komissarov, M.C. Heaven, Chem. Phys. Lett. 368 (2003) 568.
[8] A.J. Ray, R.D. Coombe, J. Phys. Chem. 99 (1995) 7849.
[9] W.W. Rice, R.J. Jensen, J. Phys. Chem. 76 (1972) 805.
[10] N. Eyet, A. Midey, V.M. Bierbaum, A.A. Viggiano, J. Phys. Chem. A 114 (2009) 1270.
[11] A.J. Midey, I. Dotan, S. Lee, W.T. Rawlins, M.A. Johnson, A.A. Viggiano, J. Phys. Chem. A 111 (2007) 5218.
[12] A.J. Midey, I. Dotan, J.V. Seeley, A.A. Viggiano, Int. J. Mass Spectrom. 280 (2009) 6.
[13] A.J. Midey, I. Dotan, A.A. Viggiano, J. Phys. Chem. A 112 (2008) 3040.
[14] A. Quinto-Hernandez, Y.-Y. Lee, T.-P. Huang, W.-C. Pan, J.J.-M. Lin, P. Bobadova-Parvanova, K. Morokuma, P.C. Samartzis, A.M. Wodtke, Int. J. Mass Spectrom. 265 (2007) 261.
[15] D.C. Frost, C.B. Macdonald, C.A. McDowell, P.C. Westwood, Chem. Phys. 47 (1980) 111.
[16] N. Eyet, K. Freel, M.C. Heaven, A.A. Viggiano, J. Chem. Phys. A 114 (2010) 6832.
[17] K. Freel, J.F. Friedman, T.M. Miller, M.C. Heaven, A.A. Viggiano, J. Chem. Phys. 132 (2010) 134308.
[18] A.A. Viggiano, R.A. Morris, F. Dale, J.F. Paulson, K. Giles, D. Smith, T. Su, J. Chem. Phys. 93 (1990) 1149.
[19] W.S. Drozdoski, A.P. Baronavski, J.R. McDonald, Chem. Phys. Lett. 64 (1979) 421.
[20] M.J. Frisch, G.W. Trucks, H.B. Schlegel, G.E. Scuseria, M.A. Robb, J.R. Cheeseman, J.J.A. Montgomery, T. Vreven, K.N. Kudin, J.C. Burant, J.M. Millam, S.S. Iyengar, J. Tomasi, V. Barone, B. Mennucci, M. Cossi, G. Scalmani, N. Rega, G.A. Petersson, H. Nakatsuji, M. Hada, M. Ehara, K. Toyota, R. Fukuda, J. Hasegawa, M. Ishida, T. Nakajima, Y. Honda, O. Kitao, H. Nakai, M. Klene, X. Li, J.E. Knox, H.P. Hratchian, J.B. Cross, V. Bakken, C. Adamo, J. Jaramillo, R. Gomperts, R.E. Stratmann, O. Yazyev, A.J. Austin, R. Cammi, C. Pomelli, J.W. Ochterski, P.Y. Ayala, K. Morokuma, G.A. Voth, P. Salvador, J.J. Dannenberg, V.G. Zakrzewski, S. Dapprich, A.D. Daniels, M.C. Strain, O. Farkas, D.K. Malick, A.D. Rabuck, K. Raghavachari, J.B. Foresman, J.V. Ortiz, Q. Cui, A.G. Baboul, S. Clifford, J. Cioslowski, B.B. Stefanov, G. Liu, A. Liashenko, P. Piskorz, I. Komaromi, R.L. Martin, D.J. Fox, T. Keith, M.A. Al-Laham, C.Y. Peng, A. Nanayakkara, M. Challacombe, P.M.W. Gill, B. Johnson, W. Chen, M.W. Wong, C. Gonzalez, J.A. Pople, Gaussian 03, Revision D.01, Gaussian, Inc., Pittsburgh, PA, 2004.
[21] L.A. Curtiss, K. Raghavachari, P.C. Redfern, V. Rassolov, J.A. Pople, J. Chem. Phys. 109 (1998) 7764.
[22] A.D. Becke, J. Chem. Phys. 98 (1993) 5648.
[23] C. Lee, W.T. Yang, R.G. Parr, Phys. Rev. B 37 (1988) 785.
[24] N. Hansen, A.M. Wodtke, A.V. Komissarov, K. Morokuma, M.C. Heaven, J. Chem. Phys. 118 (2003) 10485.
[25] J.N. Harvey, Phys. Chem. Chem. Phys. 9 (2007) 331.
[26] J.N. Harvey, M. Aschi, Phys. Chem. Chem. Phys. 1 (1999) 5555.
[27] Z. Yang, B. Eichelberger, O. Martinez, M. Stepanovic, T.P. Snow, V.M. Bierbaum, J. Am. Chem. Soc. 132 (2010) 5812.